

# Applied Improved Canny Edge Detection for Diagnosis Medical Images of Human Brain Tumors

Sarab Mohammed Taher<sup>1\*</sup>, Mustafa Ghanim<sup>2</sup>, Chen Soong Der<sup>3</sup>

<sup>1</sup>Medical Instruments Engineering, Ashur University College, Baghdad, IRAQ.

<sup>2</sup>Department of Communication Engineering, University of Technology-Iraq, Baghdad, IRAQ.

<sup>3</sup>Department of Informatics, University of Tenaga Nasional (UNITEN), Selangor, MALAYSIA.

\*Correspondent contact: [sarab.mohamed@au.edu.iq](mailto:sarab.mohamed@au.edu.iq)

## Article Info

Received  
04/05/2023

Revised  
28/06/2023

Accepted  
23/07/2023

Published  
30/12/2023

## ABSTRACT

Medical image processing has become one of the crucial elements of the diagnostic process because of the increased usage of medical imaging recently, and clinicians' dependence on such computer-processed medical images in diagnosing patients. As the traditional Canny edge detection algorithm is sensitive to noise, it is easy to lose weak edge information when filtering out the noise, and its fixed parameters show poor adaptability. The suggested algorithm introduced the concept of image block intensity operator to replace image gradient. In addition, the computing speed of the suggested algorithm is relatively fast because it works block by block rather than pixel by pixel. Two adaptive threshold selection methods are presented, one based on the median accumulative histogram of image gradient magnitude and the other on the standard deviation for both types of image pixels (one with less edge information and the other with rich edge information). The proposed algorithm can be divided into four stages: Input the medical digital image, convert the color medical image to gray-scale, applied improved canny edge detection, then calculate the MSE & PSNR Measures, in addition conduct a visual questionnaire by oncologists to find out which method that made the enhancement of the medical image clearer.

**KEYWORDS:** Medical tumors images, Median Accumulated Histogram, CED, Sobel.

## الخلاصة

أصبحت معالجة الصور الطبية أحد العناصر المهمة في عملية التشخيص نتيجة الاستخدام المتزايد للتصوير الطبي مؤخراً، واعتماد الأطباء على مثل هذه الصور الطبية المعالجة بالحاسوب في تشخيص المرضى. في هذا البحث، نقدم كشفاً محسناً للحافة يستخدم في معالجة الصور الرقمية الطبية. تعد خوارزمية Canny التقليدية للكشف عن الحواف حساسة للضوضاء، وبالتالي من السهل فقدان معلومات الحافة الضعيفة عند الفلترة، بالإضافة إلى ضعف التأقلم بسبب معاملات الثابتة، قدمت الخوارزمية المقترحة مفهوم تقسيم الصورة إلى عدد من البلوكات لاستبدال تدرج الصورة. بالإضافة إلى ذلك، فإن سرعة الحوسبة للخوارزمية المقترحة سريعة نسبياً لأنها تعمل كتلة تلو كتلة بدلاً من بكسل تلو الآخر. واختيار قيمتان من حد العتبة استناداً إلى متوسط الرسم البياني المتراكم لمقدار تدرج الصورة والانحراف المعياري لنوعين من بكسلات الصورة (أحدهما يحتوي على معلومات حافة أقل، والآخر يحتوي على معلومات حواف غنية) على التوالي. يمكن تقسيم الطريقة المقترحة إلى أربع مراحل: إدخال الصورة الرقمية الطبية، وتحويل الصورة الطبية الملونة إلى المستوى الرمادي، وتطبيق الخوارزمية المحسنة لكشف حواف الصورة، ثم حساب مقاييس MSE و PSNR، بالإضافة إلى إجراء استبيان نظري من قبل أطباء الأورام لتحديد كفاءة الخوارزمية المحسنة بالاعتماد على النتائج النظرية للصور الطبية التي تمت معالجتها مقارنة مع الخوارزميات التقليدية.

## INTRODUCTION

Image processing can be defined as an approach for the application of operations on the image for improving or extracting relevant information from it. It can be defined as a type of signal processing using an image for input, while output is either that image or its features. In the case of utilizing such visual tools, the image

analysts utilize various interpretive fundamentals [1]. In addition, digital image processing methods provide the ability of computer-assisted alterations of the digital images [2]. Preprocessing, display, enhancement, in addition to information extraction, represent the 3 general processes which all kinds of the data have to go through in

the case of utilizing digital approaches. Pixels are the picture elements that make up digital images [3][4]. Pixels are usually arranged in an ordered rectangular array. The pixel array dimensions define the image size [5] [6]. The number of columns in the array determines the width of the image, while the number of rows determines the height of the image. The pixel array is therefore a matrix with N rows and M columns. We specify the pixel's coordinates at y and x to refer to it within the image matrix [2][7][8].

In 1986, the Canny edge detection (CED) approach presented three distinct criteria, namely the signal-to-noise ratio (SNR) criterion, precision of localization criterion, and single-edge response criterion, to evaluate the effectiveness of edge detection operators. Based on these criteria, the optimal CED operator was derived [9]. In comparison to conventional edge detection algorithms, the CED algorithm generally yields superior edge detection outcomes [9]. In contemporary times, a plethora of scholars have proposed numerous enhanced algorithms utilizing the principles of the CED algorithm, which have been effectively employed within the sphere of applied engineering. Er-Sen Li enhanced the operator for computing the magnitude of image gradients and automated the edge detection process using Otsu's threshold selection method, yielding moderately positive outcomes in terms of edge detection performance [8].

In various computer vision applications, edge detection has been considered as the first step. Edge detection dramatically decreases the quantity of data in an image by filtering away insignificant or unwanted data and revealing the important information. With regard to image processing, such information is utilized for detecting objects. Medical image edge detection is a crucial preprocessing phase in medical image segmentation for the object recognition of human organs like ribs and lungs [10]. Edges define the boundaries between the image's various regions. Those boundaries are utilized to distinguish objects for the purposes of matching and segmentation. The following are the major phases in medical image edge detection:

1. **Smoothing:** this phase attempts to eliminate as much noise as possible while preserving actual edges.

2. **Enhancement:** this phase applies a filter for improving image's edge quality (i.e., sharpening).
3. **Detection:** this phase determines which pixels of the edge must be deleted as noise and which ones must be preserved (typically Thresholding presents the criterion utilized for detection).
4. **Localization:** this phase determines an edge's exact location (sub-pixel resolution could be needed for certain applications, in other words, estimate the edge's location more sufficiently than spacing between the pixels). This phase frequently necessitates edge linking and thinning [9].

### Traditional Edge Detection Techniques

Edge detection may be carried out in various methods. It can, yet, be categorized into two types, which are: Laplacian and gradient [11]. The latter finds edges through looking for minimum and maximum values in the 1st derivative of the image. To locate the edges, Laplacian approach searches for zero crossings in the 2nd derivative of the image. The most widely utilized discontinuity-based edge detection approaches, as indicated below [11-13].

#### Sobel Filter

Sobel proposed the Sobel edge detection technique in 1970 (Rafael C. Gonzalez 2004). The Sobel approach of image segmentation edge detection utilizes Sobel approximation to derivative for the purpose of discovering the edges. In addition, the Sobel filter represents a basic approximation regarding the gradient with smoothing concept. The 3 x 3 convolutional mask is typically utilized for identifying Y and X direction gradients as illustrated in Figure 1.

X – Direction Kernel			Y – Direction Kernel		
-1	0	1	-1	-2	-1
-2	0	2	0	0	0
-1	0	1	1	2	1

**Figure 1.** Masks that are utilized by Sobel operators [5].

Those kernels, one for each one of the 2 perpendicular orientations, have been developed for responding in a maximal way to edges traveling horizontally and vertically relative to the grid of pixels. The kernels could be

individually applied to input images for the purpose of providing separate measurements of the gradient component in every orientation ( $G_y$  and  $G_x$ ). The problem of this method is the absolute magnitude regarding the gradient at every point as well as its orientation can after that be specified through the combination of such results [14][15].

**Prewitt's Operator**

Prewitt can be defined as a suitable approach for the estimation of orientation and magnitude of the edge. In contrast to other approaches of gradient edge detection, requiring very time-consuming computation for estimating the direction from magnitudes in  $y$  &  $x$  directions. The problem of this method is that it is only able to go in 8 directions; however, experience has revealed that the majority of the direct estimations of the direction aren't much better. For 8 directions, such a gradient-based edge detector is estimated in a  $3 \times 3$  neighborhood as shown in Figure 2 [4][16][17].

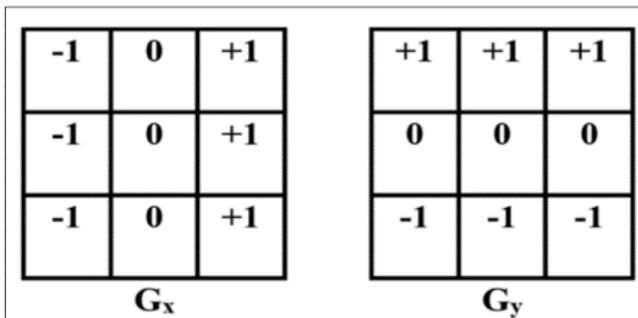


Figure 2. Masks utilized in Prewitt gradient edge detector[17].

**Robert's Cross Operator**

Lawrence Roberts is the developer of Roberts's edge detection (1965). It computes a simple 2D spatial gradient measurement on an image within a short amount of time as shown in Figure 3. This approach highlights areas with high spatial frequency that are usually corresponding to the edges. Which is why high spatial frequency regions, frequently corresponding to edges, have been highlighted. Both operator's output and input are gray-scale images in the most usual utilization. There are 22 convolution masks. The operator consists of a pair of ( $2 \times 2$ ) convolutional kernels. One of the kernels is just 90o rotated

from the other one. This is a lot like the Sobel operator [18][19].

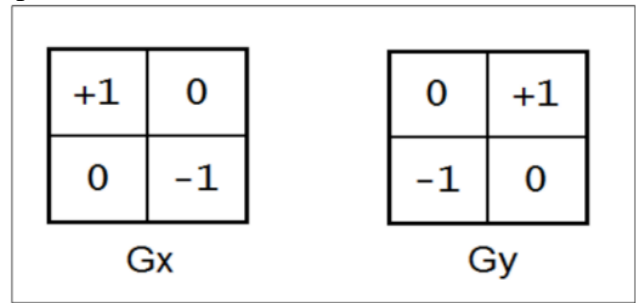


Figure 3. Masks utilized by Robert operator [3].

Those kernels, (1) for each one of the (2) perpendicular directions, have been developed for responding in a maximal way to edges running at  $45^\circ$  to pixel grid. The problem of this method is the kernels could be applied to the input image separately to provide separate measurements of gradient components in every one of the orientations ( $G_y$  and  $G_x$ ) [20][21].

**Laplacian of Gaussian**

The Laplacian of Gaussian (LOG) operator determines the best edge detection filter based on the image's SNR. To find the edges, first apply a Gaussian function to low-pass smooth the image; after that apply a high-pass filter to the Laplacian operator based on the 2nd derivative of zero. The problem of this method is that we need to discover a discrete convolutional kernel which might approximate 2nd derivatives in the formulation of Laplacian because the input image has been represented as a series of the discrete pixels [22]. Figure 4 shows the most typically utilized small kernels.

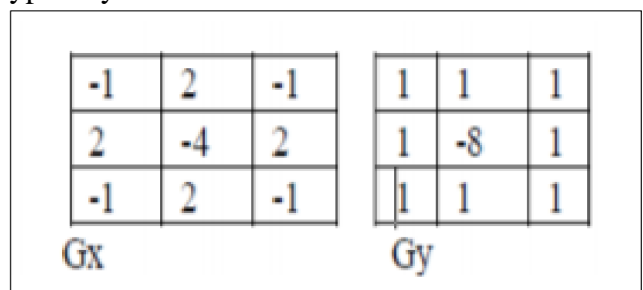


Figure 4. Mask of Laplacian filter [22].

**Traditional Canny Operator**

Edge detection, localization, and only one response to one edge are all good features of the

CED classical method. The stages taken by CED are as follows:

- To remove the noise, it first smoothed the image with the use of a Gaussian filter.
- It then uses the Sobel operator for finding the image gradient and highlighting regions.
- Followed by suppressing any pixel that isn't at maximum (non-maximum suppression).
- To follow along the remaining pixels that weren't suppressed, hysteresis is utilized. The Double Threshold approach employs two thresholds, T2 and T1, to divide gradients into 3 groups:
  - x Gradients < T1: definitely non-edge point
  - x Gradients > T2: definitely edge point
  - x Or else, the decision is made based on the point's direction and the present edge paths. Automatically determining T2 and T1 threshold values is complicated, particularly when the boundaries of the image are vague [23][24]. The traditional CED algorithm have two problems the First, conventional algorithms assume limited first-order differences of 2×2 neighboring regions to compute the image gradients [25]. A second problem is that the double threshold of the conventional CED algorithm is set to a fixed value. For images rich in edge information, the adaptability of traditional CED algorithms is not ideal, and local characteristic edge information is prone to loss.

### The Proposed Improved CED Algorithm

This paper introduced the concept of accumulated histogram to divide each region of the image into blocks by calculating the median value rather than mean value for each block in the image because of the mean value may distort for a large change in color values intensities of the block, while the median value is impervious to spurious values. The purpose of dividing image into blocks to replace the image gradient, and proposed two adaptive threshold selection methods for two kinds of medical sample images.

## MATERIALS AND METHODS

The proposed method involves four main stages applied in MATLAB in order to achieve a diagnosis of human brain tumors using improving canny edge detection. And make a comparison between the improved CED and traditional edge detection methods to find out the quality of the suggested algorithm based on the values that were

calculated by the MSE and PSNR measures. And finally applied subjective measures depending on oncologists evaluation. The proposed system is as follows:

**Stage 1:** Input RGB medical image: We use JPEG format of human brain tumor image.

**Stage 2:** Convert the color image to gray- level.

**Stage 3:** Applying improved canny edge detection:
 

- a. Smooth the image to reduce the noise by using a sobel filter.
- b. Divide image into K blocks with size U×V.
- c. The block values are arranged in ascending order, after that calculate the median value for the first block in the image by the Equation 1.

Median

$$= \left\{ B \left( \frac{n+1}{2} \right) \text{ if } (n) \text{ is odd } \frac{B \left( \frac{n}{2} \right) + \left( B \left( \frac{n}{2} \right) + 1 \right)}{2} \right\}_i \quad (1)$$

(n) represents the number of values in the block and is equal to (U × V), B (n+1/2) represents pixel value in block in location (n+1/2), B(n/2) represents pixel value in block in location (n/2).

- d. Save the values in a temporal matrix.
- e. Calculate the frequent of the median values saved in the matrix (temporal).
- f. Find the most common median. The most common median represents the number of pixels containing the same color value in the first block.
- g. Advance to the next block then repeat previous steps (secondly, fourthly). These steps continue until the last block of image.
- h. Threshold Selection Adaptive, the result of the matrix is understood as image gradient, and when the intensity on a pixel is higher than the threshold, the pixel is considered to be an edge point. The threshold for pixels is calculated based on the median of the gradient magnitude and standard deviation of the matrix image gradient, whose center is the pixel I[i,j] (N is an odd number, generally larger than 20). Then, the threshold value of the pixel can be obtained by Equation 2.

$$E_v = \frac{\sum_{i=1}^m \sum_{j=1}^n |E[i,j]|}{(m * n)} \quad (2)$$

When the pixel I [i, j] is in the image's border region and the matrix is less than N×N, the incorrect parts are set to null, and the median and standard deviation of this matrix were used to calculate the threshold. As a result, each pixel

has its own double threshold, and the entire image's edge information may be acquired by detecting and connecting edges. Algorithm 1 depicts the key stages of the improved CED algorithm.

**Algorithm: Improved CED.**

**Input:** Medical Colored Image.

**Output:** Shape Boundary of Medical Image

**Step1:** Read RGB Medical image.

**Step2:** Convert RGB into Grey-level.

**Step3:** Divide the medical image into K blocks, k=4 with 2 × 2 size.

**Step4:** Calculate a median value for the first block and save these values in a temporal matrix.

**Step 5:** Calculate the median values frequently and find the most median value frequent.

**Step 6:** Create the first block based on the blocks that contain the most frequent median values.

**Step 7:** Move to the next block and repeat steps from 2 to 4. And continue until complete the last block of the medical image.

**Step 8:** Adaptive Threshold Selection.

**Step 9:** Calculate MSE & PSNR to measure the quality of the resulting edge image.

**End.**

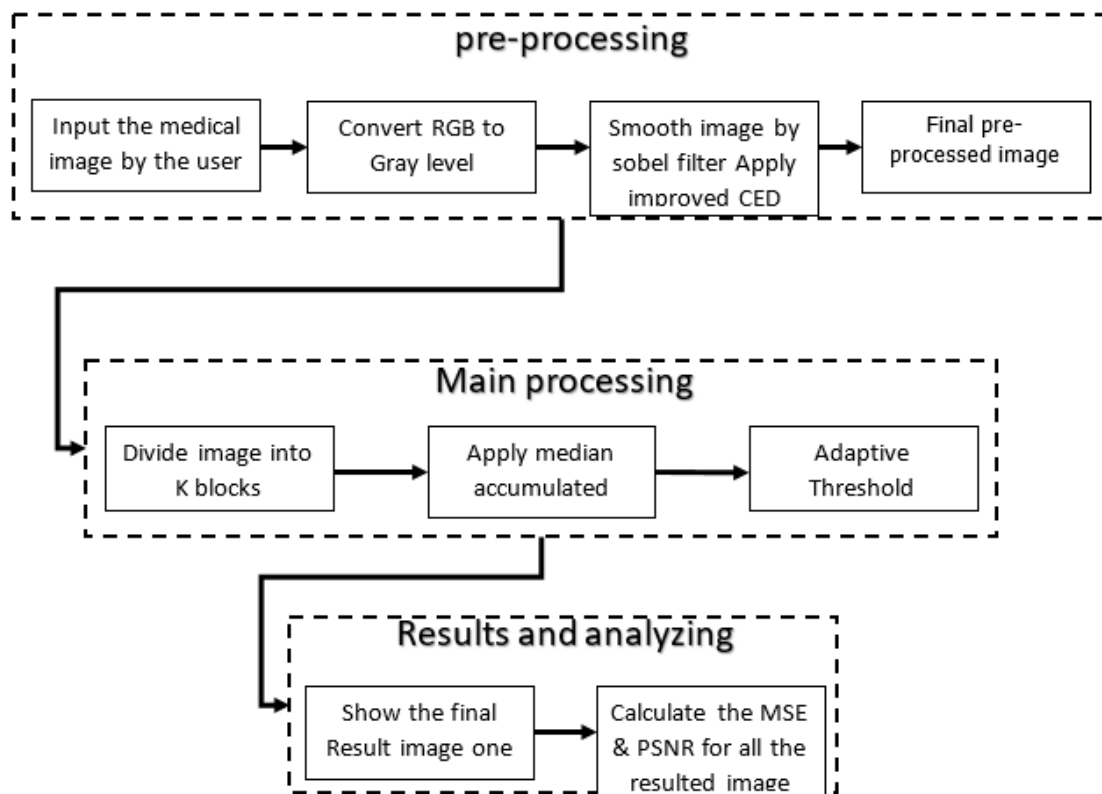
**Stage 4:** Make a comparison between the proposed improved CED and the traditional methods (Sobel Filter, Prewitt Filter, Roberts Filter, Laplacian Filter, and traditional Canny algorithm) using PSNR and MSE to get the error ratio of the resulting medical image for each method. The MSE represents the total difference between the original and compressed image. MSE reduces error and enhances image quality when used in small amounts. The smaller the MSE, the better image's edge quality. MSE is defined as follows:

$$MSE = \frac{1}{mn} \sum_{i=0}^{m-1} \sum_{j=0}^{n-1} [I(i, j) - K(i - j)]^2 \quad (3)$$

where PSNR is most easily defined via the mean Squared Error (MSE). The bigger the PSNR, the better the edge quality of the resulting image. The PSNR (in dB) is defined as:

$$PSNR = 10 \log_{10} \frac{(2^n - 1)^2}{\sqrt{MSE}} \quad (4)$$

Figure 5. explains the overall block diagram of the suggested method.



**Figure 5.** The block diagram of the Improved CED algorithm.

## RESULTS AND DISCUSSION

The case study in the proposed method is implemented and tested using MATLAB on two samples of human brain tumor images which are 256-level gray for each sample, in order to identify medical image tumors. The results from figures (6-9) & table (1-3) illustrates the major stages of the suggested approach. Beginning from input the RGB image (brain tumor), convert the color image to gray-level, applying the improved CED and the traditional edge detection methods on gray image (Sobel Filter, Prewitt Filter, Roberts Filter, and Laplacian Filter, traditional CED) one after another for each sample of medical image, and compute the MSE & PSNR Measures the quality of the improved CED.

Depending on the measures of PSNR & MSE in Table 1 and 2 that show an improved CED algorithm is better than the traditional methods, and then Prewitt Filter, Sobel Filter, Roberts Filter, and then Laplacian Filter in ascending order.

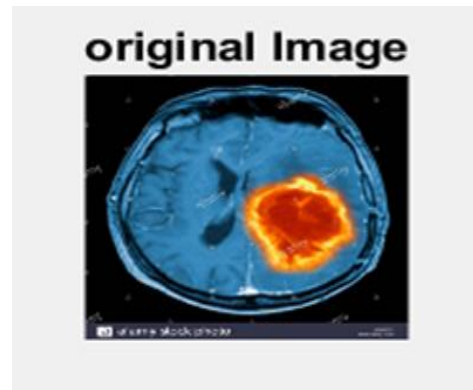


Figure 6. The process of input RGB brain tumors image.

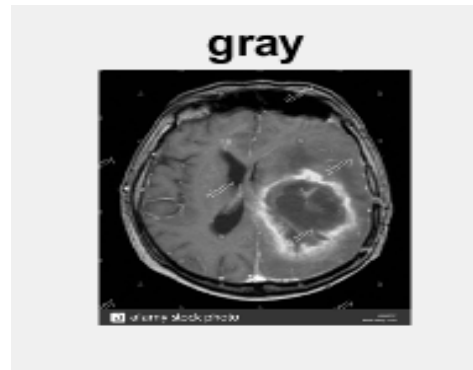


Figure 7. Convert RGB medical image into gray-level.

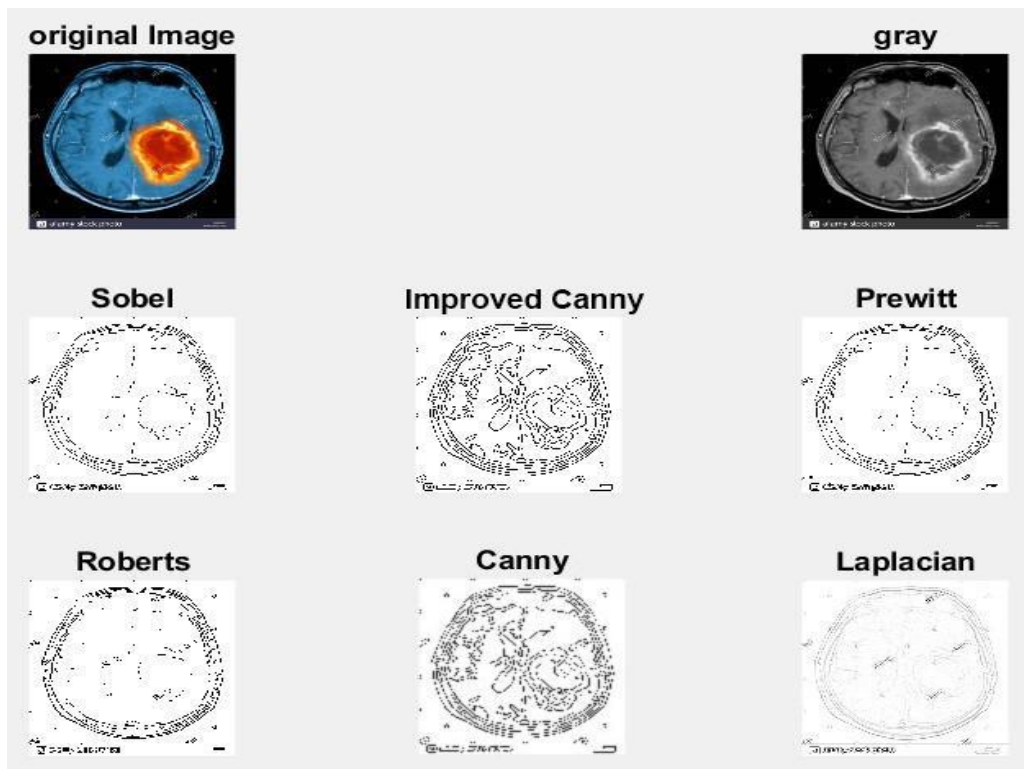
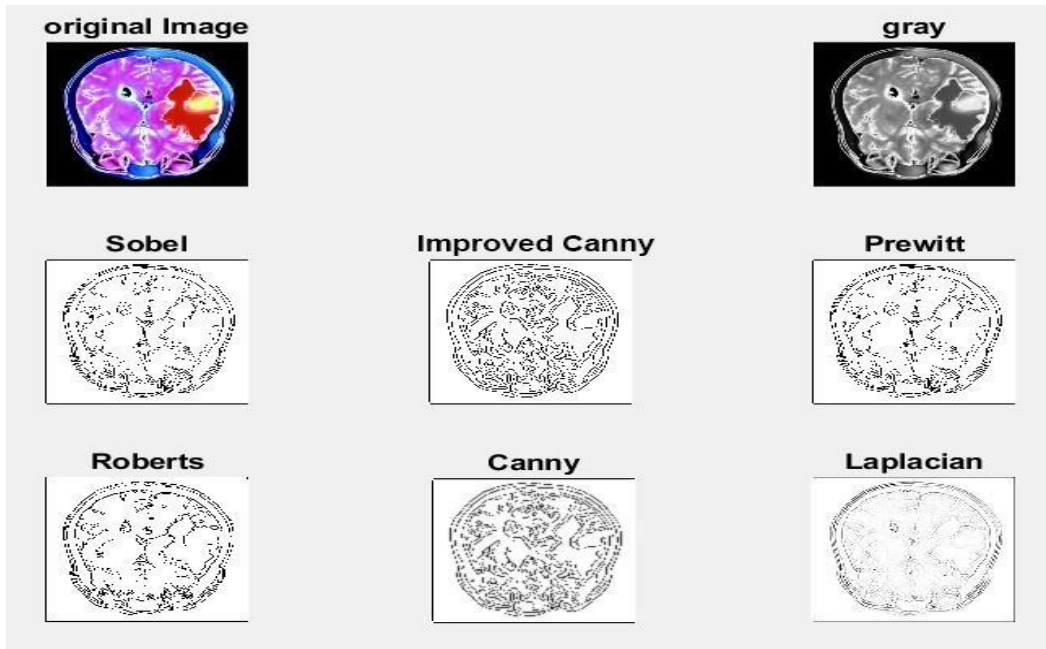

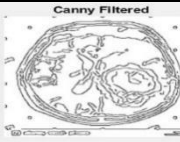
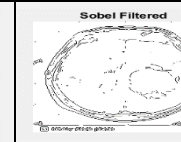
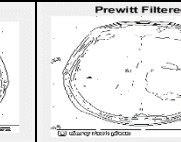
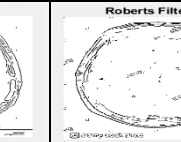
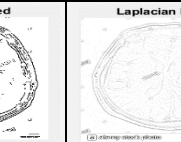


Figure 8. Results after applying improved CED & traditional method on 1<sup>st</sup> sample of brain tumors image.

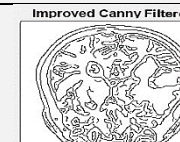
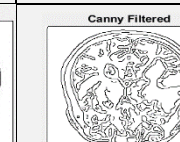
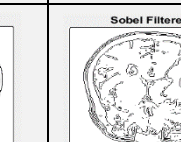
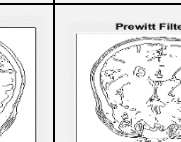
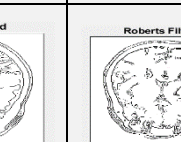
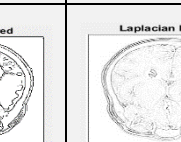


**Figure 9.** Results after applying improved CED & traditional method on 2<sup>nd</sup> Sample of Brain Tumors Image.

**Table 1.** The output results of the MSE & PSNR measurements for the 1<sup>st</sup> Medical Image sample.

MSE Values	Improved CED	Traditional CED	Sobel	Prewitt	Roberts	Laplacian
	2.5345e+04	3.7645e+04	6.9872e+03	6.9868e+03	6.9877e+03	6.9957e+03
PSNR Values	9.8722	9.3737	7.6878	7.5880	5.7875	5.6825
1st sample						

**Table 2.** The output results of the MSE & PSNR measurements for the 2<sup>nd</sup> Medical Image sample.

MSE Values	Improved CED	Traditional CED	Sobel	Prewitt	Roberts	Laplacian
	0.4269e+04	1.5272e+04	4.5265e+04	4.5264e+04	4.5267e+04	3.0108e+04
PSNR Values	9.7918	9.39405	6.2918	6.2941	6.1132	4.3440
2 <sup>nd</sup> sample						

**Table 3.** The Subjective Measure of 1<sup>st</sup> & 2<sup>nd</sup> samples.

Oncologists Opinion of 1 <sup>st</sup> & 2 <sup>nd</sup> sample	Improved CED	Traditional CED	Sobel	Prewitt	Roberts	Laplacian
1 <sup>st</sup> Oncologist	✓	✓				
2 <sup>nd</sup> Oncologist	✓	✓				
3 <sup>rd</sup> Oncologist	✓					
4 <sup>th</sup> Oncologist	✓			✓		
5 <sup>th</sup> Oncologist		✓				
6 <sup>th</sup> Oncologist	✓					
7 <sup>th</sup> Oncologist	✓		✓			
8 <sup>th</sup> Oncologist	✓	✓				
9 <sup>th</sup> Oncologist	✓			✓		

Table 3 explains the oncologist's evaluation of subjective measure, a questionnaire was conducted for 9 oncologists to know their opinion about the best method that gives more accurate details to help them in the process of diagnosing a brain tumor. Where the eight oncologists found the result of improved CED in 1<sup>st</sup> & 2<sup>nd</sup> samples is very efficient than other filters because it visually gives more details about the tumor image that has been entered, which helps them in the diagnosis process more accurately.

## CONCLUSIONS

This study emphasizes the diagnosis of human brain tumors and aims to assist the medical community in utilizing computer image processing techniques for more accurate diagnostic outcomes. The proposed enhanced algorithm initiates by segmenting the image region into 2×2 blocks, prioritizing computational speed over individual pixel intensity calculations simultaneously. Instead of employing the mean value susceptible to distortion from significant shifts in color value intensities within the block, two adaptive thresholds are chosen through median accumulated histogram analysis.

This algorithm focuses on edge identification in medical images by initially smoothing the image and removing noise. Subsequently, an enhancement process is implemented to achieve higher image quality. A comparison among five filters was conducted to determine the most effective filter based on objective metrics such as MSE and PSNR measures. Moreover, subjective evaluations were conducted by nine Oncologists to ascertain the filter's performance.

**Disclosure and Conflict of Interest:** The authors declare that they have no conflicts of interest.

## REFERENCES

- [1] S. Chen and C. Shao, "Efficient online tracking-by-detection with kalman filter," *IEEE Access*, vol. 9, pp. 147570-147578, 2021. <https://doi.org/10.1109/ACCESS.2021.3124705>
- [2] S. Hazim and A. Kharofa, "Remove Noise from Medical Images Digital images enhancement View project Remove Noise from Medical Images," 2018. [Online]. Available: <https://www.researchgate.net/publication/331175763>
- [3] F. A. Pellegrino, W. Vanzella, and V. Torre, "Edge detection revisited," *IEEE Transactions on Systems, Man, and Cybernetics, Part B: Cybernetics*, vol. 34, no. 3, pp. 1500-1518, Jun. 2004. <https://doi.org/10.1109/TSMCB.2004.824147>
- [4] M. F. A. Kadir, A. F. A. Abidin, M. A. Mohamed, and N. A. Hamid, "Spam detection by using machine learning based binary classifier," *Indonesian Journal of Electrical Engineering and Computer Science*, vol. 26, no. 1, pp. 310-317, Apr. 2022. <https://doi.org/10.11591/ijeecs.v26.i1.pp310-317>
- [5] L. Andersson and C. Peng, "Comparison of Anti-Aliasing in Motion Contact Information," 2018. [Online]. Available: [www.bth.se](http://www.bth.se)
- [6] R. Biswas and J. Sil, "An Improved Canny Edge Detection Algorithm Based on Type-2 Fuzzy Sets," *Procedia Technology*, vol. 4, pp. 820-824, 2012. <https://doi.org/10.1016/j.protcy.2012.05.134>
- [7] S. Bhardwaj and A. Mittal, "A Survey on Various Edge Detector Techniques," *Procedia Technology*, vol. 4, pp. 220-226, 2012. <https://doi.org/10.1016/j.protcy.2012.05.033>
- [8] F. Başçiftçi and E. Avuçlu, "Determination age and gender with edge detection algorithms using dental X-ray images," *El-Cezeri Journal of Science and Engineering*, vol. 7, no. 1, pp. 315-321, 2020. <https://doi.org/10.31202/ecjse.646581>
- [9] Sarab Mohammed Taher; Mustafa Ghanim, "Applied Augmented Reality in Entertainment with Behavior and Geometry Consistency," 2022.
- [10] W. McIlhagga, "The canny edge detector revisited," *Int J Comput Vis*, vol. 91, no. 3, pp. 251-261, Feb. 2011. <https://doi.org/10.1007/s11263-010-0392-0>
- [11] T. Rahman Talukdar, M. J. Hossain, and T. H. Talukdar, "Malaria detection in Segmented Blood Cell using Convolutional Neural Networks and Canny Edge Detection."
- [12] F. Alkhalid, "Online Preprocessing of Gesture Signs Using Background Substructure and Edge Detection Algorithms," *International Journal of Simulation Systems Science & Technology*, Mar. 2020. <https://doi.org/10.5013/IJSSST.a.21.02.02>
- [13] G. Guo and N. Razmjoooy, "A new interval differential equation for edge detection and determining breast cancer regions in mammography images," *Systems Science and Control Engineering*, vol. 7, no. 1, pp. 346-356, Jan. 2019. <https://doi.org/10.1080/21642583.2019.1681033>
- [14] H. Kumar Buddha, P. Kumar Bammidi, B. Harish, R. Sagar, B. H. Kumar, and B. Pradeep Kumar, "Crack Identification in Railway Track Using Edge detection method Internet of Things View project Optical communication View project Crack Identification in Railway Track Using Edge detection method," 2020. [Online]. Available: <https://www.researchgate.net/publication/342872375>
- [15] R. Dutt Sharma and S. Kumar Gupta, "A Survey on Moving Object Detection and Tracking Based On Background Subtraction," *The Oxford Journal of Intelligent Decision and Data Science*, vol. 2018, pp. 55-62, 2018. <https://doi.org/10.5899/2018/ojids-00041>



- [16] M. K. Ikram, Y. T. Ong, C. Y. Cheung, and T. Y. Wong, "Retinal vascular caliber measurements: Clinical significance, current knowledge and future perspectives," *Ophthalmologica*, vol. 229, no. 3, pp. 125-136, Apr. 2013.  
<https://doi.org/10.1159/000342158>
- [17] G. T. Shrivakshan and C. Chandrasekar, "A Comparison of various Edge Detection Techniques used in Image Processing," 2012. [Online]. Available: [www.IJCSI.org](http://www.IJCSI.org)
- [18] M. Gandhi, J. Kamdar, and M. Shah, "Preprocessing of Non-symmetrical Images for Edge Detection," *Augmented Human Research*, vol. 5, no. 1, Dec. 2020.  
<https://doi.org/10.1007/s41133-019-0030-5>
- [19] V. Tyagi, *Understanding Digital Image Processing*. CRC Press, 2018.  
<https://doi.org/10.1201/9781315123905>
- [20] B. Saha Tchinda, D. Tchiotsop, M. Noubom, V. Louis-Dorr, and D. Wolf, "Retinal blood vessels segmentation using classical edge detection filters and the neural network," *Inform Med Unlocked*, vol. 23, Jan. 2021.  
<https://doi.org/10.1016/j.imu.2021.100521>
- [21] G. Guo and N. Razmjoo, "A new interval differential equation for edge detection and determining breast cancer regions in mammography images," *Systems Science and Control Engineering*, vol. 7, no. 1, pp. 346-356, Jan. 2019.  
<https://doi.org/10.1080/21642583.2019.1681033>
- [22] M. Harahap, A. C. Wijaya, S. H. H. Pasaribu, G. Sembiring, and K. C. Ginting, "Edge Detection Of Potato Leaf Damage With Laplacian Of Gaussian Algorithm," *Sinkron*, vol. 7, no. 3, pp. 1054-1058, Aug. 2022.  
<https://doi.org/10.33395/sinkron.v7i3.11583>
- [23] W. McIlhagga, "The canny edge detector revisited," *Int J Comput Vis*, vol. 91, no. 3, pp. 251-261, Feb. 2011.  
<https://doi.org/10.1007/s11263-010-0392-0>
- [24] Z. Stosic and P. Rutesic, "An Improved Canny Edge Detection Algorithm for Detecting Brain Tumors in MRI Images." [Online]. Available: <http://iaras.org/iaras/journals/ijsp>
- [25] R. Biswas and J. Sil, "An Improved Canny Edge Detection Algorithm Based on Type-2 Fuzzy Sets," *Procedia Technology*, vol. 4, pp. 820-824, 2012.  
<https://doi.org/10.1016/j.protcy.2012.05.134>

## How to Cite

S. M. Taher, M. . Ghanim, and C. S. Der, "Applied Improved Canny Edge Detection for Diagnosis Medical Images of Human Brain Tumors", *Al-Mustansiriyah Journal of Science*, vol. 34, no. 4, pp. 66–74, Dec. 2023.

